

# Highly sensitive detection of low abundant molecules by pyro-electrohydro-dynamic jetting

Romina Rega<sup>1</sup>, Martina Mugnano<sup>1</sup>, Danila del Giudice<sup>1</sup>, Simona Itri<sup>1</sup>, Volodymyr Tkachenko<sup>1</sup>, Veronica Vespini<sup>1</sup>, Sara Coppola<sup>1</sup>, Emanuela Mazzon<sup>2</sup>, Emilia Oleandro<sup>1,3</sup>, Pierangelo Orlando<sup>1</sup>, Pietro Ferraro<sup>1</sup> and Simonetta Grilli<sup>1</sup>

<sup>1</sup>*Institute of Applied Sciences and Intelligent Systems of CNR, Pozzuoli (NA), Italy*

<sup>2</sup>*IRCCS “Bonino Pulejo”, Messina, Italy*

<sup>3</sup>*University “Luigi Vanvitelli”, Caserta, Italy*

## Abstract

The effective detection of low-concentrated molecules in small volumes represents a significant challenge in many sectors such as biomedicine, safety, and pollution. Here, we show an easy way to dispense liquid droplets from few  $\mu\text{l}$  volume (0.2-0.5  $\mu\text{l}$ ) of a mother drop, used as reservoir, by using a pyro-hydrorodynamic jetting (p-jet) dispenser. This system is proposed for multi-purpose applications such as printing viscous fluids and as a biosensor system. The p-jet system is based on the pyroelectric effect of polar dielectric crystals such as lithium niobate (LN). The electric field generated by the pyroelectric effect acts electro-hydrodynamically on the sample of liquid, allowing the deposition of small volumes. The p-jet approach allows to obtain the dispensing of drops of very small volumes (up to tenths of a picoliter) avoiding the use of syringes and nozzles generally used in standard technologies. The reliability of the technique as a biosensor is demonstrated both in the case of oligonucleotides and in a sample of clinical interest, namely gliadin. The results show the possibility of detecting these biomolecules even when they are low abundant, i.e. down to attomolar. The results show a marked improvement in the detection limit (LOD) when compared with the conventional technique (ELISA). Moreover, it has been presented the possibility of using the p-jet as a useful tool in the detection of biomarkers, present in the blood but currently not detectable with conventional techniques and related to neurodegenerative diseases such as Alzheimer.

## Introduction

The ability to manipulate and dispense liquids on a micro and nanometric scale allows important benefits in many fields such as combinatorial chemistry, printing applications, and biotechnology. On the other side, the development of increasingly performing and innovative sensors is now the prerogative of research of the most advanced laboratories in the world [1-4]. In particular, the ability to detect biomolecules in very low concentrations has repercussions in various areas such as biomedicine, pollution, forensic activity etc. [3,4]. Hence, there is a constantly growing demand for

specific tools for the deposition of ultra-small quantities of materials in predefined places in order to develop miniaturized instruments for the fabrication of highly integrated and automated "lab-on-a-chip" systems based on microfluidics [5,6]. The ability to fabricate complex microfluidic architectures has allowed scientists to create new highly efficient experimental formats for fast processing of small analytical volumes, thus resulting in reduced reagent consumption and extremely low manufacturing costs. Moreover, greater operational flexibility and the possibility of integrating functional components within complex analytical schemes give the additional benefit of greater portability of the instruments. Currently, most microfluidic systems consist of microchannels in which liquids are manipulated by applying pressure or voltage variations to the electrodes thus involving some disadvantages such as complex manufacturing, cross-contamination of the sample and the need to apply high voltages or pressures. In recent years, conventional approaches such as microcontact printing [7], photolithography [8], nanoimprint [9], and direct laser writing [10] have been overcome by inkjet printing, that exhibits numerous advantages in terms of flexibility, high precision and controllability of nanomaterials patterns in nanofabrication and nanodevices [11]. In particular, Electrohydrodynamic jet (E-jet) printing is widely used in important applications, such as biosensors [12], micro-nano optical devices [13], and flexible electronic devices [14].

Here we show a simple system in which the manipulation and dispensing of the liquid is obtained through an 'electrode-free' configuration based on the physical properties of a dielectric crystal such as the Lithium Niobate-LiNbO<sub>3</sub> (LN). The technique, defined as "pyroelectrodynamic dispenser jet" (p-jet), allows to deposit both separate drops with lower volumes than traditional systems, and printing fiber of viscous fluids [15-17]. This technique is based on the dispensing induced by means of an electric field generated by the pyroelectric effect from LN crystal subjected to a temperature gradient. P-jet allows to manipulate liquids in a no-contact mode and avoids the use of nozzles and external electrodes thus overcoming some severe limitation of ink-jet printing, ie nozzle clogging [18]. Recently, p-jet approach was used for different applications, including, accumulation of very diluted biomolecule [19,20], the formation of spiral fibers [21] and manipulation of soft matter [15-17]. We show the main applications of this technology starting from the manipulation and printing of viscous fluids to the develop of a sensor capable of detecting low concentrations of molecules otherwise not detectable with conventional technologies. In this framework, the efficiency of the p-jet based biosensor for the detection of oligonucleotides and gliadin protein was demonstrated. The usefulness of the p-jet based biosensor can be extended to any field in which the detection of low concentration quantities is required, such as the case of biomarker in the blood (currently not detectable with the technologies available on the market) which represents the alarm bell of the presence of some neurodegenerative disease such as Alzheimer's disease (AD). Therefore, the p-jet proves to be a useful, low cost and easy to implement tool that paves the way for the early diagnosis of many silent diseases.

## **Experimental**

### **Lithium niobate**

The lithium niobate (LN) crystals were purchased from Crystal Technology Inc. and were in the form of 500  $\mu\text{m}$  thick and 3-inch diameter wafers with both sides polished and mono-domain ferroelectric state.

## Pyroelectric effect

LN with cut  $c$  is a ferroelectric crystal is characterized by pyroelectric properties, therefore, at room temperature, it has a spontaneous polarization  $P_s$  conventionally oriented from the so-called face  $c$  to face  $c^+$ . At equilibrium, if it is not thermally stimulated, the polarization charge of the LN crystal is completely screened from external screening charges on the surface of the crystal and no electric field is generated. The thermal stimulation induces a change of  $P_s$  as a consequence, a transient electrostatic state appears with screening charges not compensated on the crystal surface. According to the pyroelectric effect, this phenomenon is associated with a high electric field that originates from the surface of the crystal [22-24]. This electric field can be used for a wide range of applications ranging from biological to soft matter manipulation [25-29].

## P-jet system

Fig.1 shows a schematic view of the p-jet set-up.

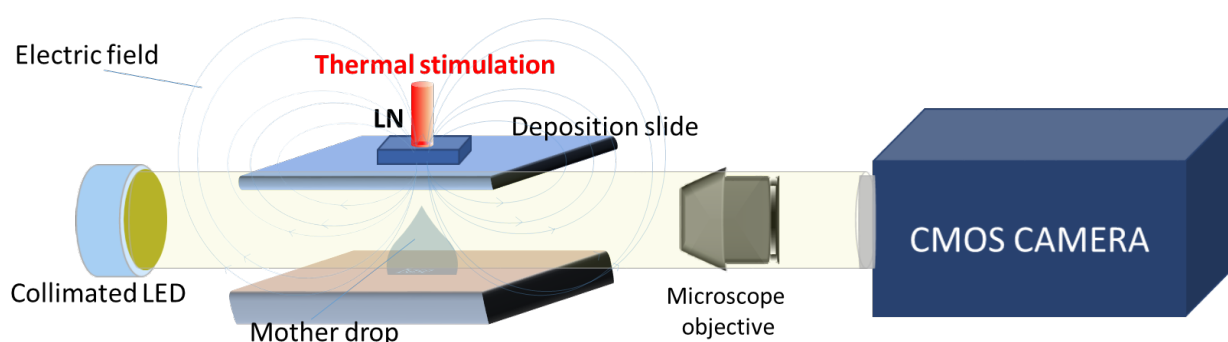


Figure 1: Schematic view of the p-jet system, the electric field is schematized by grey lines.

A conventional optical path consisting of a collimated LED, an optical microscope objective (10 $\times$ ) and a high-speed CMOS camera (Motion Pro Y3-S1, pixel size of 10.85 $\times$ 10.85  $\mu\text{m}^2$ ). These instruments allow us to have a side view of the experiment during the dispensing events. The p-jet set-up consists of a basic support that hosts the liquid sample, manually deposited, that we will call here "mother drop" (eg 0.2  $\mu\text{L}$  volume), while the dispensing slide, that represents the target support where the deposition occurs, faces parallel and is mounted on a motorized translation system. The pyroelectric crystal is placed above the dispensing slide substrate. The temperature gradient is induced in the crystal by direct contact with a heating instrument that can be a conducting wire heater (heated by Joule effect), or a hot tip of a common soldering iron or without contact using a laser source that emits in the far-infrared (CO<sub>2</sub> laser,  $\lambda = 10.3 \mu\text{m}$  wavelength falls within the absorption band of the LN crystals). The pyro-electrohydrodynamic effect consists of charge displacement induced in the mother drop due to the electric field, pyroelectrically generated (in Figure 1 the field it is schematized by grey lines), that employs attractive and repulsive forces to the liquid molecules [30,31].

Figures 2 (a) and 2 (b) schematically show the side view of the configuration of the mother drop. Neglecting the effect of gravity, the mother drop has a hemispherical shape with a static contact angle  $\theta$  defined by the mechanical equilibrium of three interfacial tensions: liquid vapour ( $\sigma_{lv}$ ), solid vapour ( $\sigma_{sv}$ ) and solid-liquid ( $\sigma_{sl}$ ) interface tensions, respectively. Following a thermal stimulation, the LN generates an electric field that surrounds the mother drop which deforms due to the effect of the electrical, capillary and viscous forces, as shown schematically in Fig. 2 (b). Charges accumulate on the surface, and the drop assumes a conical profile called "Taylor cone". This conical shape is maintained up to a certain critical limit of the electric potential [32]. Once that limit is exceeded, the profile of the meniscus can no longer be supported by the surface tension, and the fluid will be ejected from the apex of the cone. The electric field produces an electrostatic polarization stress that causes the initial deformation of the drop, therefore, the fluid will be ejected from the cone when the electrostatic stresses overcome the surface tension [33-35].

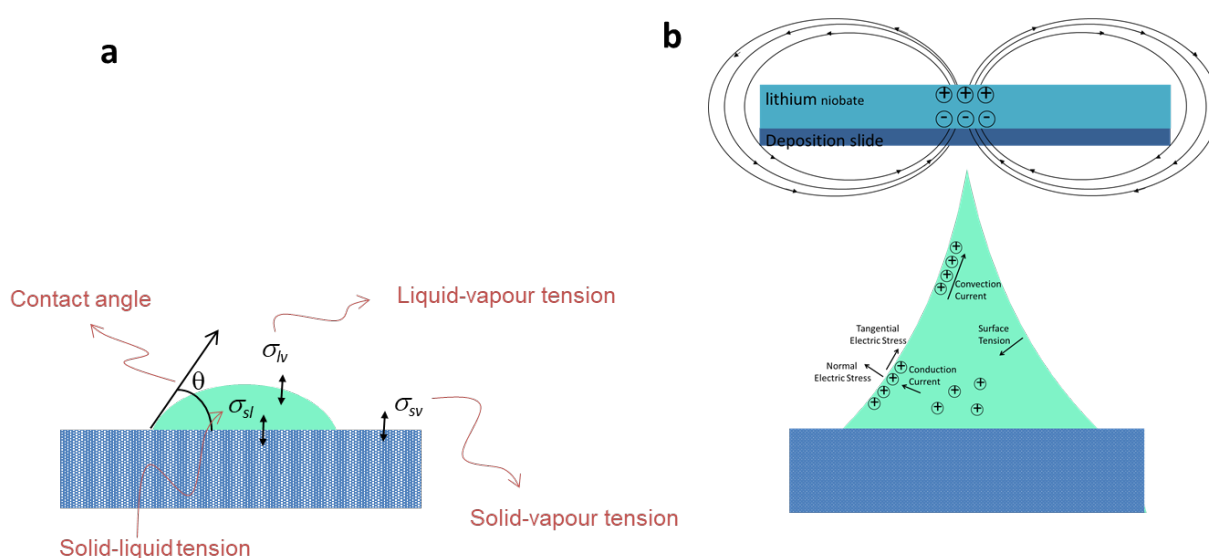


Figure 2: Schematic view of (a) the base drop under the equilibrium condition and of (b) the base drop in presence of the pyroelectric field.

## Test analytes

5'-Cy5 ( $\lambda_{ex}$ -650 nm;  $\lambda_{em}$ -670 nm) fluorescence-labelled oligonucleotide (5'-CGCGATCCCACCCAGGGAGCCACTGAGATGATGGCG-3', 66.7% G-C content, MW 12,131  $\text{gmol}^{-1}$ ) was synthesized at Eurofins mwg/ operon—Ebersberg-D. region. The oligonucleotide was solubilized in Tris-EDTA buffer at initial concentration of 100 mM. A 300-nM stock solution was prepared and serial dilutions in Tris-EDTA were used. The samples were mixed with an advanced buffer system (Micro-Spotting Solution Plus 2X, ArrayIt), in a ratio 1:1, to improve the surface properties of the oligonucleotide samples deposited during printing. The analyte solution (0.2 ml) was deposited onto the base support by a Hamilton Modified Microliter Syringe (7000 Series). 1 mg of gliadin was solubilized in 1ml of phosphate-buffered saline and 0.1M sodium bicarbonate solution was added to raise the pH of the reaction mixture to 8–8.5. A volume of 100 ml of solution was labelled using the Alexa Fluor 647 Antibody Labelling Kit (Molecular Probes, Invitrogen) following the manufacturer's instructions. The reaction mixture was loaded onto a spin column (available with the kit), containing a gel filtration resin in phosphate-buffered saline (pH 7.2), and after centrifugation

at 1,100g for 5min, the labelled protein (~100 ml) was collected in a tube, while the band of unreacted dye was retained in the void volume. The concentration of labelled gliadin (610 ng ml<sup>-1</sup>) was calculated measuring the adsorbance at 280 nm and subtracting the adsorbance at 650 nm corrected by a 0.03 factor, to eliminate the contribution of lysine-linked dye.

### **Fluorescence scanner**

A conventional fluorescence scanner InnoScan 710 (Innopsys, Carbonne, France) was used for reading the slides. Main scan parameters: laser source at 530 nm and 10mW power; pixel size 3 mm and scan speed of 10 lines s<sup>-1</sup>; detection gain 25% PMT

## **Results and discussions**

### **The p-jet for liquid printing**

The p-jet configuration allows printing various liquids, such as viscous fluids. Given the volume (V) of the mother drop, which acts as a mother drop, and its contact angle ( $\theta$ ), depending on the type of liquid and the substrate, a critical distance value  $D_C$ , between the mother drop and the deposition slide, can be defined:

$$D_C = (1 + \theta / 4) V^{1/3}$$

According to this equation, it is possible to distinguish two different conditions: (1) for distances shorter than  $D_C$  a stable liquid bridge is generated and it is therefore possible to print a strip of fluid continuously by translation of the dispensing slide; (2) for distances larger than  $D_C$ , an instability situation develops and small daughter droplets will be thrown from the mother drop. Therefore, this instability is used to dose and dispense liquids [34]. The p-jet system can be used as a printing tool directly to the desired substrate by break the mother drop in secondary droplets to be delivered as separate single drops or having a continuous deposition of the fluid strip starting from the mother drop.

We are able to print different geometries by controlling the direction of translation and the speed of the deposition slide and droplets and lines of liquids with extremely regular diameters and widths and according to a wide variety of geometries. Figure 3 shows some simple patterns printed by oleic acid, almond oil and mineral oil in separate droplets, straight and curved lines.

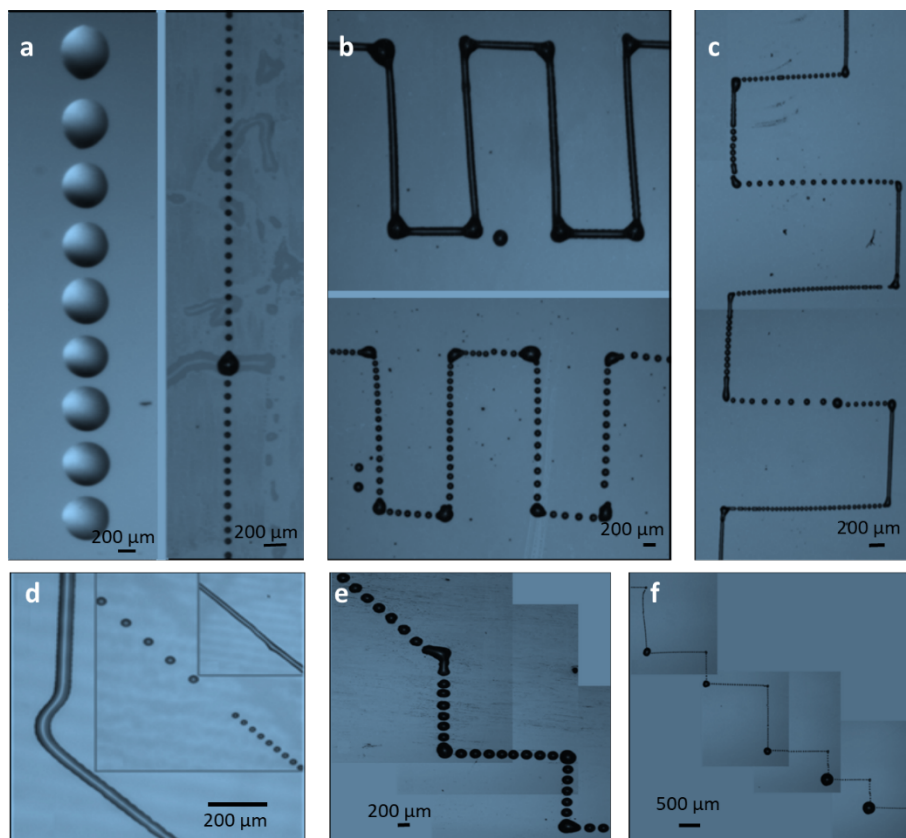


Figure 3: Some example of patterns printed by oleic acid, almond oil and mineral oil in separate droplets, straight and curved lines: a), Linear array of periodic separate droplets printed by almond oil (top) and mineral oil (bottom) (diameter, 15 mm). b) Continuous (top) and dotted (bottom) printed by mineral oil. c) Continuous and dotted patterned by almond oil. d) Simple patterns printed by oleic acid: separate droplets (diameters, 40 and 25 mm), straight and curved lines (width, 40 mm). e) Dotted staircase including a non-orthogonal angle. Staircase with smaller droplets (25 mm) printed with large vertices by almond oil. f), Dotted staircase with small vertices (droplet diameter, 30 mm) printed by oleic acid.

The revolutionary feature of p-jet is to avoid the use of the deposition tools traditionally used in printing protocols (i.e. syringes, nozzles), thus performing much easier and faster dosing procedures.

### The p-jet for accumulating biomolecules

The reliability and the multi-purpose capability of the p-jet technique was demonstrated for biosensing application. The p-jet system is able to detect low abundant biomolecules by guiding and accumulating biomolecules in the mother drop directly onto the surface of a functionalized deposition slide. The key concept of this type of approach is called “split and stack”. The biomolecules are dispensed on a small area of the deposition slide and this occurs thanks to the possibility of split the mother drop through a series of very small droplets and stuck them in a limited area of the receiving substrate. Using labelled biomolecules, with this approach, it is possible to increase the density of the fluorescence signal and improve significantly the sensitivity. Furthermore, the classic diffusion phenomena, encountered in conventional detection techniques such as ELISA, are avoided [36]. The comparison between the two approach is schematized in fig 4.

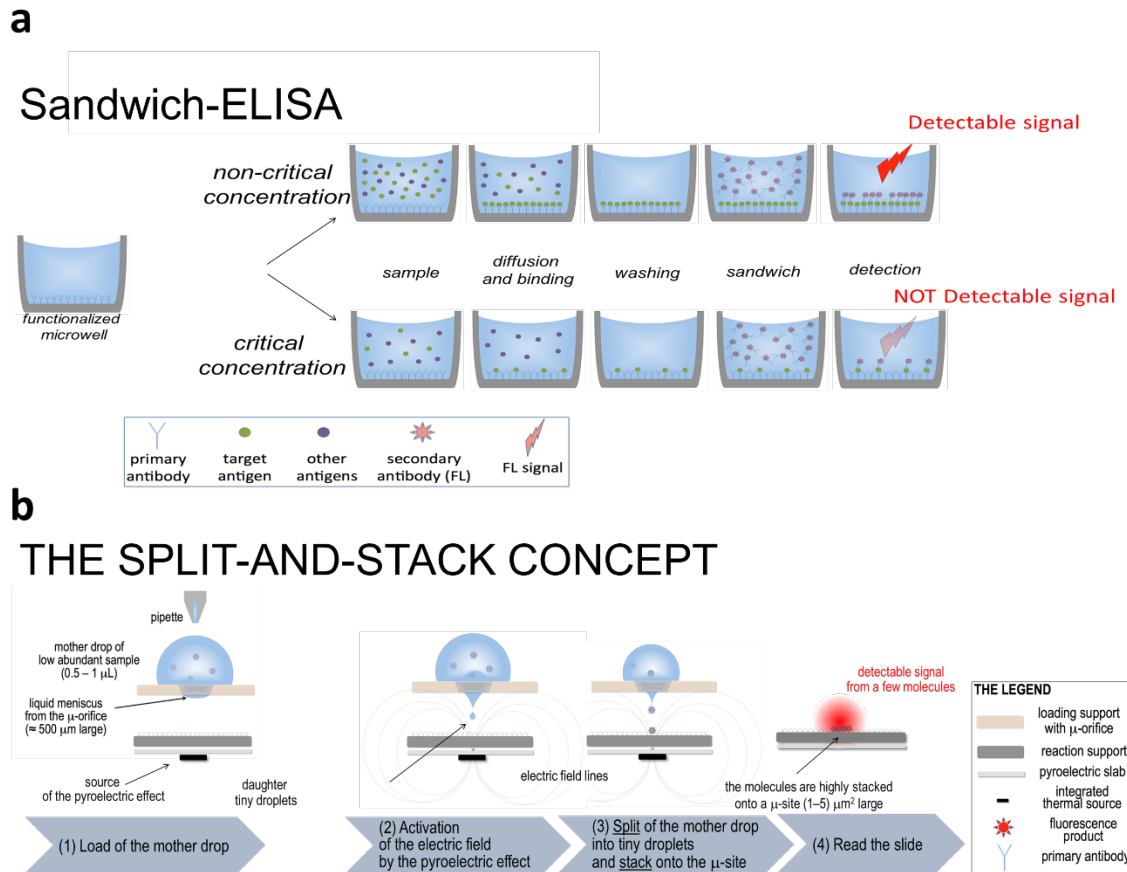


Figure 4: Schematic view of the accumulation effect. (a) in standard ELISA deposition: manual dispensing of the drop into a petri dish used in the ELISA kit; b) in p-jet accumulation approach

The coloured dots represent the target molecules and other antigens in a solution, while the Y symbols indicate the binding molecules on the deposition slide (SuperAmmine, Super Nylon, ArrayIt). We focus here on a sample solution with critical concentration, namely well below the values corresponding to the LOD of standard ELISA kits (tens of pg/mL). Moreover, for the sake of simplicity, we hypothesize here that the reaction between deposition slide and binding molecules produces a fluorescent (FL) spot. The well-based reaction (ELISA kit) is shown in Fig.4(a) while the p-jet based reaction is shown in Fig.4(b). In the first case, an appropriate incubation time makes the target molecules to diffuse into the reaction volume (100  $\mu$ L) up to encountering the binding molecules on the well surface. However, due to a relatively high discrepancy between volume reaction and molecule concentration, the bound products are distributed over a relatively large surface, thus producing a FL signal per unit area very weak with a bad signal-to-noise ratio (SNR) that makes the molecules un-detectable. Conversely, the p-jet allows us to deliver the same amount of molecules onto a confined area of the target slide ( $\sim 1\div 5 \mu\text{m}^2$ ) thus forcing the target molecules to react with binding ones into a reduced volume. As a consequence, the FL signal per unit area is much higher, the SNR increases significantly and those few molecules become detectable.



## Oligonucleotides detection

The ability of the system to concentrate the analytes has been deepened by comparing the fluorescence signal of the p-jet spots and that of the spots obtained by depositing the same sample volume with a standard pipette. As first test, we used a stock solution of a single strand (SS, single strand) DNA oligonucleotide (15-20 bases) at 300 nM concentration labeled with Cy5 (fluorophore emitting in the red region  $\lambda_{\text{ex}} \sim 650 \text{ nm}$ ;  $\lambda_{\text{em}} \sim 670 \text{ nm}$ ). Successive dilutions from that solution were prepared. Serial dilutions, between 300 nM and 300 aM have been analyzed, and Figure 5 (a) shows how by depositing the drop in the classical way, the fluorescence signal decays with decreasing concentration. The limit of detection (LOD) was calculated using a value three times the intensity of the standard deviation of the background. Figure 5 (b) shows the result of the scan in the case of four different concentrations of DNA solutions spotted with the two methods. The concentration effect of the signal is clearly visible through an increase in the fluorescence of the spot obtained by p-jet of about 95% compared to the standard spot where is evident the diffusion phenomena in each spot.

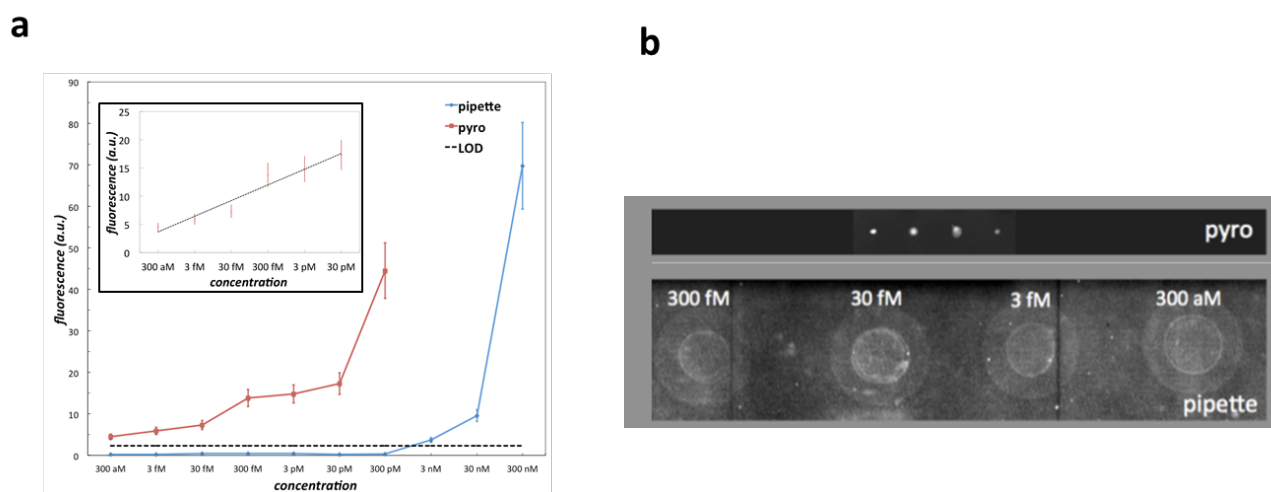


Figure 5: Quantitative evaluation of the oligonucleotide spots. Plot of (a) mean fluorescence and b) Typical scanner scan for the four spots, corresponding to the concentrations indicated in the image, in the case of multiple and subsequent spots obtained with p-jet (upper); classical deposition with pipettes (down). Each scan refers to concentrations (from left to right) of 300 fM, 30 fM, 3 fM, 300 aM, respectively.

## Gliadin detection

The performance of the p-jet for detecting low abundant molecules was tested also in case of a protein of clinical interest, the gliadin. Gliadin represents the predominant protein component in gluten. The presence of gluten in food must be kept under control by people with celiac disease who follow a gluten-free diet. In the European Union, a maximum level of 20 p.p.m. of gluten is allowed for a product declared "gluten-free". To date, the presence of gluten in food is usually detected by conventional ELISA tests [37]. As already said, this technology shows diffusion limits that do not allow the detection of biomolecules when they are in very low concentration. Therefore, a reliable and highly sensitive technique for evaluating the gluten content in foods it would be of great benefit to patients, dieters and food producers.



The p-jet was used to detect different concentrations of gliadin labelled by Alexa Fluor 647 (240pg / ml; 120pg / ml; 24pg / ml; 12 pg / ml; 1 pg / ml). Figure 6a shows the fluorescence signal of the spots obtained with p-jet technology as a function of the dilution factor of gliadin, while Fig. 6b shows the corresponding fluorescence profiles and scanner images of the spots obtained with the p-jet system. The results clearly show that the p-jet system can efficiently detect 1 pg of gliadin in 0.2  $\mu$ l of solution (0.005 p.p.m.), thus achieving a 60-fold improvement over the current ELISA test limits (0.3 p.p.m.) [38].

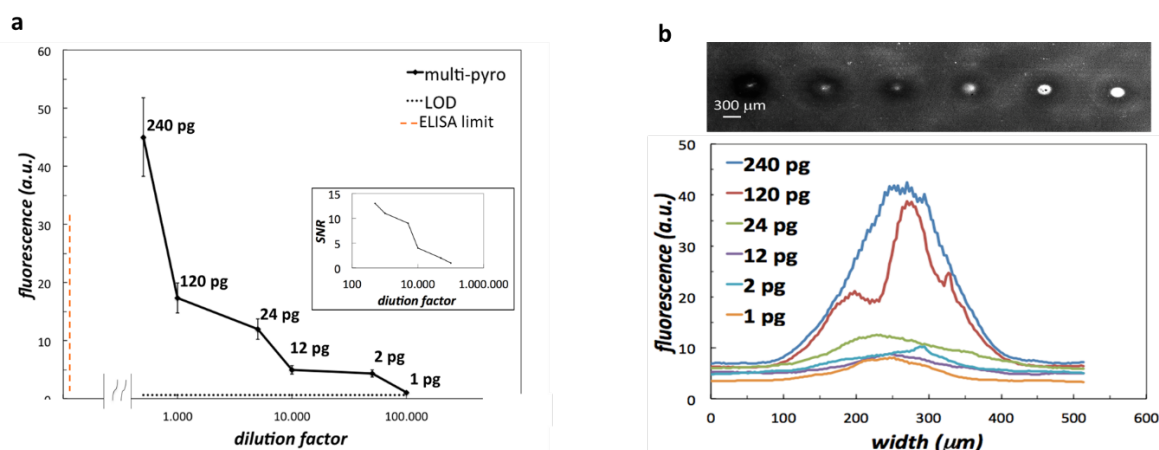


Figure 6. Quantitative evaluation of the gliadin spots. (a) Plot of fluorescence of the gliadins spotted by the p-jet, as a function of the dilution factor and corresponding linearity curve. (b) Mean fluorescence profiles of the gliadins spots obtained with p-jet system and corresponding scanner image where the dilution grows from top to bottom.

### AD biomarker

In the framework of biosensors, the detection of biomarkers present in very low concentrations in the blood could have significant implications in the early diagnosis of some diseases, especially in the neurological field as in case of the Alzheimer's disease [39]. The current guidelines for clinical diagnosis of AD establish the determination of specific protein biomarkers (Amyloid-beta, tau, P-tau) in cerebrospinal fluid (CSF) through ELISA kit and the positron emission tomography (PET) of the brain with amyloid tracer. This procedure, besides being invasive for the patient, requires hospitalization and qualified personnel, and, moreover the disease is diagnosed when has progressed massively. Nowadays the traditional ELISA kits cannot determine such biomarkers in peripheral blood due to their abundance well below his LOD of 50-100 pg/mL. This detection limit (LOD) is due to the diffusion phenomena encountered by antigens and antibodies due to the large reaction volumes (50-100  $\mu$ L) in relatively large areas (1/5 mm<sup>2</sup>), leading to a significant lowering of the signal / noise ratio.

The use of p-jet as biosensor allows us to detect small traces in the blood (concentration below 1pg / mL) of protein biomarkers of AD. In order to overcome the ELISA LOD, the biosensor aims to concentrate micro-droplets of the biological sample, containing the biomarkers of interest, on a very restricted area of a deposition slide chemically bonding the biomarker with its antibody. Thus the diffusion problems are avoided because the reaction between the biomarker (antigen) and the respective antibody is maximized, thus maximizing the probability of encounter, thus increasing the fluorescence signal per unit area. The volumes to be used are clearly lower than those used in standard

technology, in fact 0.2  $\mu\text{L}$  of biological sample containing the biomolecules of interest (marked in fluorescence) are deposited manually by an operator on a support that acts as a mother drop. The deposition slide is chemically functionalized with the antibody (antibody specific to the biomolecule to be detected) and placed as showed schematically in Fig.4 (b). After thermal stimulation, it follows on that a pyro-electric field appears capable of dividing the mother drop into many small micro-drops which will be accumulated in a single site of micrometric dimension on the functionalized deposition slide. Therefore, the reaction will be forced with a high efficiency since the diffusion phenomena will be cancelled obtaining much stronger fluorescence signals. The authors are leading the European Project 'SensApp' funded under the H2020 program and aiming at developing a super-sensor able to detect AD biomarkers by a simple blood test [40]. Thanks to this approach it will possible to develop a simple and inexpensive test to identify a biomarker panel directly in a drop of blood where the concentration of biomolecules indicative of the disease is very low. Therefore, it will be possible to carry out an early diagnosis of AD and easy screening among the population.

## Conclusion

The innovative pyro-electrodynamic jet (p-jet) method has been used as a printing device for viscous fluids and for applications as a biosensor. The p-jet is based on the hydro-electrodynamic effect on the fluid, generated by an electric field activated pyroelectrically by a lithium niobate crystal. The performances of the p-jet have been tested for the rapid and extremely sensitive detection of oligonucleotides and gliadin protein. The operating principle is extremely simple and effective. A mother drop containing the biomolecules to be detected is split into many small droplets and stacked in a limited area of the deposition slide, in this way, the diffusion phenomena that limit the detection of low abundant molecules are eliminated and therefore sensitivity is increased.

Furthermore, this innovative system is extremely versatile since it can also be used (following appropriate adaptations) to identify biomarkers present in very low concentrations in the blood related to pathologies such as Alzheimer's disease. It is easy to predict the social impact of this advanced technology, since, as in the case of AD disease, which has a high incidence and is currently without a cure, its early diagnosis would lead to an advanced study of the disease in the early stages of human beings and therefore the identification of possible treatments. Furthermore, the technique is extremely simple and inexpensive and absolutely non-invasive for the patient. Hospitalization and withdrawal of the patient's spinal fluid with very delicate procedures that require specialized and qualified personnel is not necessary. This technology will enable faster and non-invasive early diagnosis of diseases in the future simply through routine blood tests, thus paving the way for highly efficient screening programs among the population. In summary, this multipurpose technology opens the way to all those applications where the manipulation of small volumes of fluids is necessary and the need to detect low abundant molecules with important repercussions in the diagnostic field.

## Funding

The authors acknowledge the EU funding within the Horizon 2020 Program, under the FET-OPEN Project SensApp, Grant Agreement No. 829104.

## References

- [1] Mandracchia, B., Palpacuer, J., Nazzaro, F., Bianco, V., Rega, R., Ferraro, P., & Grilli, S. (2018). Biospeckle decorrelation quantifies the performance of alginate-encapsulated probiotic bacteria. *IEEE Journal of Selected Topics in Quantum Electronics*, 25(1), 1-6.
- [2] Bianco, V., Mandracchia, B., Nazzaro, F., Rega, R., Ferraro, P., & Grilli, S. (2019). Detection of self-propelling bacteria by speckle correlation assessment and applications to food industry. In *Optical Methods for Inspection, Characterization, and Imaging of Biomaterials IV* (Vol. 11060, p. 1106007). International Society for Optics and Photonics.
- [3] Fraden, J. (2016). Chemical and Biological Sensors. In *Handbook of Modern Sensors* (pp. 645-697). Springer, Cham.
- [4] Beniwal, A., Srivastava, V., & Sharma, S. (2019). Sol-gel assisted nano-structured SnO<sub>2</sub> sensor for low concentration ammonia detection at room temperature. *Materials Research Express*.
- [5] Zheng, B., Tice, J. D., Roach, L. S., & Ismagilov, R. F. A droplet-based, composite PDMS/glass capillary microfluidic system for evaluating protein crystallization conditions by microbatch and vapor-diffusion methods with on-chip X-ray diffraction. *Angewandte chemie international edition*, 43(19), 2508-2511, (2004).
- [6] Mirasoli, M., Guardigli, M., Michelini, E., & Roda, A. (2014). Recent advancements in chemical luminescence-based lab-on-chip and microfluidic platforms for bioanalysis. *Journal of pharmaceutical and biomedical analysis*, 87, 36-52.
- [7] Gunawan, C. A., Ge, M., & Zhao, C. (2014). Robust and versatile ionic liquid microarrays achieved by microcontact printing. *Nature communications*, 5(1), 1-8.
- [8] Hung, A. M., Micheel, C. M., Bozano, L. D., Osterbur, L. W., Wallraff, G. M., & Cha, J. N. (2010). Large-area spatially ordered arrays of gold nanoparticles directed by lithographically confined DNA origami. *Nature nanotechnology*, 5(2), 121.
- [9] Hwang, B., Shin, S. H., Hwang, S. H., Jung, J. Y., Choi, J. H., Ju, B. K., & Jeong, J. H. (2017). Flexible plasmonic color filters fabricated via nanotransfer printing with nanoimprint-based planarization. *ACS applied materials & interfaces*, 9(33), 27351-27356.
- [10] Seo, B. H., Youn, J., & Shim, M. (2014). Direct laser writing of air-stable p-n junctions in graphene. *ACS nano*, 8(9), 8831-8836.
- [11] Rim, Y. S., Bae, S. H., Chen, H., De Marco, N., & Yang, Y. (2016). Recent progress in materials and devices toward printable and flexible sensors. *Advanced Materials*, 28(22), 4415-4440.
- [12] Shigeta, K., He, Y., Sutanto, E., Kang, S., Le, A. P., Nuzzo, R. G., ... & Rogers, J. A. (2012). Functional protein microarrays by electrohydrodynamic jet printing. *Analytical chemistry*, 84(22), 10012-10018.
- [13] An, B. W., Kim, K., Lee, H., Kim, S. Y., Shim, Y., Lee, D. Y., ... & Park, J. U. (2015). High-resolution printing of 3D structures using an electrohydrodynamic inkjet with multiple functional inks. *Advanced materials*, 27(29), 4322-4328.
- [14] Ding, Y., Zhu, C., Liu, J., Duan, Y., Yi, Z., Xiao, J., ... & Yin, Z. (2017). Flexible small-channel thin-film transistors by electrohydrodynamic lithography. *Nanoscale*, 9(48), 19050-19057.
- [15] Mecozzi, L., Gennari, O., Coppola, S., Olivieri, F., Rega, R., Mandracchia, B., ... & Grilli, S. (2018). Easy Printing of High Viscous Microdots by Spontaneous Breakup of Thin Fibers. *ACS applied materials & interfaces*, 10(2), 2122-2129.
- [16] Rega, R., Gennari, O., Mecozzi, L., Pagliarulo, V., Bramanti, A., Ferraro, P., & Grilli, S. (2019). Maskless arrayed nanofiber mats by bipolar pyroelectrospinning. *ACS applied materials & interfaces*, 11(3), 3382-3387.

- [17] Mecozzi, L., Gennari, O., Rega, R., Battista, L., Ferraro, P., & Grilli, S. (2017). Simple and rapid bioink jet printing for multiscale cell adhesion islands. *Macromolecular bioscience*, 17(3), 1600307.
- [18] Nie, Z., & Kumacheva, E. (2008). Patterning surfaces with functional polymers. *Nature materials*, 7(4), 277-290.
- [19] Grilli, S., Miccio, L., Gennari, O., Coppola, S., Vespini, V., Battista, L., ... & Ferraro, P. (2014). Active accumulation of very diluted biomolecules by nano-dispensing for easy detection below the femtomolar range. *Nature communications*, 5, 5314.
- [20] Rega, R., Martinez, J. M., Mugnano, M., Oleandro, E., Gennari, O., Orlando, P., ... & Grilli, S. (2019). A pyroelectric-based system for sensing low abundant lactose molecules. In *Optical Methods for Inspection, Characterization, and Imaging of Biomaterials IV* (Vol. 11060, p. 1106009). International Society for Optics and Photonics.
- [21] Mecozzi, L., Gennari, O., Rega, R., Grilli, S., Bhowmick, S., Gioffrè, M. A., ... & Ferraro, P. (2016). Spiral formation at the microscale by  $\mu$ -pyro-electrospinning. *Soft matter*, 12(25), 5542-5550.
- [22] Bhowmick, S., Iodice, M., Gioffrè, M., Breglio, G., Irace, A., Riccio, M., ... & Coppola, S. (2017). Investigation of pyroelectric fields generated by lithium niobate crystals through integrated microheaters. *Sensors and Actuators A: Physical*, 261, 140-150.
- [23] Rega, R., Gennari, O., Mecozzi, L., Grilli, S., Pagliarulo, V., & Ferraro, P. (2016). Bipolar patterning of polymer membranes by pyroelectrification. *Advanced Materials*, 28(3), 454-459.
- [24] Rega, R., Gennari, O., Mecozzia, L., Grilli, S., Pagliarulo, V., & Ferraro, P. (2016, May). Pyro-electrification of polymer membranes for cell patterning. In *AIP Conference Proceedings* (Vol. 1736, No. 1, p. 020042). AIP Publishing LLC.
- [25] Pagliarulo, V., Gennari, O., Rega, R., Mecozzi, L., Grilli, S., & Ferraro, P. (2018). Twice electric field poling for engineering multiperiodic Hex-PPLN microstructures. *Optics and Lasers in Engineering*, 104, 48-52.
- [26] Gennari, O., Marchesano, V., Rega, R., Mecozzi, L., Nazzaro, F., Fratianni, F., ... & Ferraro, P. (2018). Pyroelectric effect enables simple and rapid evaluation of biofilm formation. *ACS applied materials & interfaces*, 10(18), 15467-15476.
- [27] Gennari, O., Rega, R., Mugnano, M., Oleandro, E., Mecozzi, L., Pagliarulo, V., ... & Ferraro, P. (2019). A skin-over-liquid platform with compliant microbumps actuated by pyro-EHD pressure. *NPG Asia Materials*, 11(1), 1-8.
- [28] Rega, R., Gennari, O., Mecozzi, L., Pagliarulo, V., Mugnano, M., Oleandro, E., ... & Grilli, S. (2019). Pyro-electrification of freestanding polymer sheets: a new tool for cation-free manipulation of cell adhesion in vitro. *Frontiers in chemistry*, 7.
- [29] Lettieri, S., Rega, R., Pallotti, D. K., Gennari, O., Mecozzi, L., Maddalena, P., ... & Grilli, S. (2017). Direct evidence of polar ordering and investigation on cytophilic properties of pyroelectrified polymer films by optical second harmonic generation analysis. *Macromolecules*, 50(19), 7666-7671.
- [30] López-Herrera, J., Popinet, S. & Herrada, M. A charge-conservative approach for simulating electrohydrodynamic two-phase flows using Volume-Of-Fluid. *J Comput Phys.* 230, 1939–1955 (2011).
- [31] Zeleny, J. (1917). Instability of electrified liquid surfaces. *Physical review*, 10(1), 1.
- [32] Taylor, G. I. (1964). Disintegration of water drops in an electric field. *Proceedings of the Royal Society of London. Series A. Mathematical and Physical Sciences*, 280(1382), 383-397.
- [33] Melcher, J. R., & Taylor, G. I. (1969). Electrohydrodynamics: a review of the role of interfacial shear stresses. *Annual review of fluid mechanics*, 1(1), 111-146.

- [34] Ferraro, P., Coppola, S., Grilli, S., Paturzo, M., & Vespini, V. (2010). Dispensing nano–pico droplets and liquid patterning by pyroelectrodynamic shooting. *Nature nanotechnology*, 5(6), 429-435.
- [35] Gennari, O., Battista, L., Silva, B., Grilli, S., Miccio, L., Vespini, V., ... & Ferraro, P. (2015). Investigation on cone jetting regimes of liquid droplets subjected to pyroelectric fields induced by laser blasts. *Applied Physics Letters*, 106(5), 054103.
- [36] Shena, M. (ed. Biotechniques Books: Microarray Biochip Technology, 1st edn (Eaton Publishing Company, 2000).
- [37] Clark, M. F., Lister, R. M., & Bar-Joseph, M. (1986). ELISA techniques. In *Methods in enzymology* (Vol. 118, pp. 742-766). Academic Press.
- [38] Bugyi, Z., Török, K., Hajas, L., Adonyi, Z., Popping, B., & Tömösközi, S. (2013). Comparative study of commercially available gluten ELISA kits using an incurred reference material. *Quality Assurance and Safety of crops & foods*, 5(1), 79-87.
- [39] Hardy, J. (2006). Alzheimer's disease: the amyloid cascade hypothesis: an update and reappraisal. *Journal of Alzheimer's disease*, 9(s3), 151-153.
- [40] SensApp. SensApp <http://www.sensapp.eu/>.